Detecting mountain pine beetle red attack damage with EO-1 Hyperion moisture indices

JOANNE C. WHITE[1], NICHOLAS C. COOPS[2], THOMAS HILKER[2], MICHAEL A. WULDER[1]*, ALLAN L. CARROLL[1]

[1]Canadian Forest Service (Pacific Forestry Centre), Natural Resources Canada, 506 West Burnside Road, Victoria, British Columbia, Canada V8Z 1M5

[2]Department of Forest Resource Management, University of British Columbia, 2424 Main Mall, University of British Columbia, Vancouver, British Columbia, Canada V6T 1Z4

*Corresponding author:
Pacific Forestry Centre, 506 West Burnside Road, Victoria, British Columbia, Canada V8Z 1M5;
Phone: 250-363-6090; Fax: 250-363-0775; Email: mwulder@nrcan.gc.ca

Pre-print of published version.

Reference:
White, J.C., N.C. Coops, T. Hilker, M.A. Wulder, A.L. Carroll, 2007; Detecting mountain pine beetle red attack damage with EO-1 Hyperion moisture indices, International Journal of Remote Sensing. Vol. 28, No. 10, pp. 2111-2121.

DOI.
http://dx.doi.org/10.1080/01431160600944028

Running head:

Hyperion detection of insect attack with moisture indices

Abstract

The mountain pine beetle (*Dendroctonus ponderosae*) is the most destructive insect of mature pine forests in western North America. Time series of wetness transformations generated from Landsat imagery have been used to detect mountain pine beetle red attack damage over large areas. With the recent availability of high spatial (QuickBird) and high spectral (Hyperion) resolution satellite sensor imagery, the relationship between spectral moisture indices and levels of red attack damage may be investigated. Six moisture indices were generated from Hyperion data and were compared to the proportion of the Hyperion pixel having red attack damage. Results indicate the Hyperion moisture indices incorporating both the SWIR and NIR regions of the electromagnetic spectrum concurrently, such as the Moisture Stress Index, were significantly correlated to levels of damage (r^2=0.51; p=0.0001). The results corroborate the hypothesis that changes in foliage moisture resulting from mountain pine beetle attack are driving the broad-scale temporal variation in Landsat derived wetness indices. Furthermore, the results suggest that Hyperion data may be used to map low levels of mountain pine beetle red attack damage over large areas that are not consistently captured with Landsat data.

Keywords: mountain pine beetle, red attack, detection, Hyperion, QuickBird

1. Introduction

The total area impacted by mountain pine beetle (*Dendroctonus ponderosae*) in the province of British Columbia, Canada, increased from 164,000 ha in 1999 to 8.5 million ha in 2005 (British Columbia Ministry of Forests and Range 2005). Adult beetles typically attack the primary host, lodgepole pine (*Pinus contorta*), in August and lay eggs, which complete their development cycle into mature adults approximately one year later (Amman and Cole 1983). A synthesis of our present knowledge of mountain pine beetle biology is provided in Safranyik and Carroll (2006).

Immediately following an attack by mountain pine beetle, the foliage of trees remains visibly unchanged; however, a drop in sapwood moisture has been measured as a consequence of the attack (Reid 1961, Yamaoka *et al*. 1990). Once a tree is killed by mountain pine beetle it will initially retain its green foliage (typically called the green attack stage). Generally, the foliage fades from green to yellow to red over the spring and summer following attack (Amman 1982, Henigman *et al.* 1999), gradually desiccates, and pigment molecules breakdown (Hill *et al.* 1967). Twelve-months after being attacked, over 90% of the killed trees will have red needles (red attack). Three years after being attacked, most trees will have lost all needles (gray attack) (British Columbia Ministry of Forests 1995, Wulder *et al.* 2006a). The variability in the nature and rate of the change in foliage colour often confounds detection efforts.

Detection of red attack damage at the landscape level is generally accomplished using aerial overview surveys (Wulder *et al.* 2006a). More detailed surveys using helicopters and ground crews are then subsequently undertaken (Wulder *et al.* 2006b). Aerial photography and high spatial resolution satellite sensor imagery have been used to accurately detect and map red attack damage at the level of individual forest stands and trees (Roberts *et al*. 2004, White *et al.* 2005, Coops *et al.* 2006). White *et al.* (2005) used

IKONOS imagery to detect red attack damage with accuracies of 70.1% for areas of low infestation (stands with less than 5% of trees damaged) and 92.5% for areas of moderate infestation (stands with between 5% and 20% of trees damaged). Roberts *et al.* (2004) used scanned airborne photography to detect mountain pine beetle red attack damage with accuracies ranging between 80 and 90%. Coops *et al.* (2006) used a ratio of red to green reflectance, generated from QuickBird multispectral data, to identify red attack tree crowns. The relationship between the number of red attack pixels and observed red attack crowns was assessed using independent validation data and was found to be significant ($r^2 = 0.48$, $p < 0.001$, standard error = 2.8 crowns).

Over large areas, Landsat Thematic Mapper (TM) and Enhanced Thematic Mapper (ETM+) have been used to detect and map red attack damage at the landscape scale with 81% accuracy in areas where the damage occurs in large, contiguous patches (30-50 red attack trees) (Skakun *et al.* 2003). Mountain pine beetle red attack damage was detected using the difference between the Kauth and Thomas Tasseled Cap (TCT) wetness component (Kauth and Thomas 1976; Crist and Cicone 1984) calculated for two image dates, referred to as the Enhanced Wetness Difference Index (EWDI) (Skakun *et al.* 2003). Collins and Woodcock (1996) were the first to characterize forest mortality using the difference between wetness components generated for two dates of TM imagery. The differences in the wetness component were ideally suited to capture change in the SWIR portions of the spectrum, where the change associated with conifer mortality was likely to manifest as an increase in reflectance (due to a decrease in water absorption).

The success of the EWDI as an indicator of red attack damage is related to its ability to discriminate changes in SWIR reflectance, which can be associated with changes in foliage moisture. The availability of hyperspectral remote sensing imagery, with increased spectral resolution in terms of the number and width of the spectral bands in the visible, near-infrared (NIR, 0.7 –1.3 μm), and shortwave infrared (SWIR, 1.300–2.500 μm) regions of the electromagnetic spectrum, facilitates an investigation of the underlying assumptions associated with the EWDI. The results of this investigation could then be used to assess the continued use of the EWDI as a reliable method for detecting and mapping mountain pine beetle red attack damage at the landscape level. In this study, we evaluate the potential of Hyperion, an imaging spectrometer on the Earth Observing 1 (EO-1) satellite platform, to detect mountain pine beetle red attack damage using moisture indices. The performance of Hyperion data is evaluated by direct comparison of Hyperion-derived foliage moisture indices to estimates of red attack damage generated from QuickBird multispectral imagery.

2. Study Area

The study site is located near Merritt, British Columbia, Canada, centered at 49.84º N and 120.75º W. From 2002 to 2005, regular field surveys were conducted in three forest stands in the study area to monitor mountain pine beetle population dynamics. The amount of red attack damage increased markedly between 2003 and 2004; in stand B (Figure 1), there were 6 red attack trees/ha in 2003, increasing to 24 red attack trees/ha in 2004.

3. Data

3.1 QuickBird Imagery

High spatial resolution QuickBird imagery was acquired over the study area on July 20, 2005. The imagery was geocorrected to base planimetric data using a 1st order polynomial cubic convolution (RMS 0.4 m for the panchromatic and RMS 0.9 m for the multispectral). The imagery was acquired with a close to nadir view angle (11.4º) and a high sun elevation of 58.3º. QuickBird imagery contains four multi-spectral bands at 2.44 m spatial resolution: 0.45 - 0.52µm (blue); 0.52 - 0.60µm (green); 0.63 - 0.69µm (red); 0.76 - 0.90µm (near infra-red), and a panchromatic band (0.45- 0.90µm) with a 0.68 m spatial resolution (Birk *et al.*, 2003).

3.2 *Hyperion Data*

EO-1 was part of NASA's New Millennium Program, implemented to validate new technologies for remote sensing (Ungar *et al.* 2003) and was launched in November 2000, with an orbit following that of the Landsat-7 satellite. The EO-1 payload carried the Hyperion hyperspectral sensor, consisting of two push-broom imaging spectrometers, designed to cover the visible near-infrared (VNIR) and SWIR regions of the spectrum (Pearlman *et al*. 2003). Hyperion data has a 30 m spatial resolution and 10 nm spectral resolution ranging from 0.43 to 2.4 µm. A single date of Hyperion data was acquired from the USGS Center for Earth Resource Observation and Science (EROS) data centre. The imagery was collected on August 19, 2005 at level 1R (radiometrically corrected), which includes spectral calibration, smearing and echo correction, use of a bad pixel mask, and alignment of the VNIR and SWIR channels. Common to all Hyperion imagery is evidence of streaks which were corrected by statistical balancing using the means and variances of the columns of the data image (Coops *et al.* 2003, Datt *et al.* 2003). The Fast Line-of-sight Atmospheric Analysis of Spectral Hypercubes (FLAASH) (Matthew *et al.* 2000) algorithm was used to correct the imagery for atmospheric effects. The image was then rectified to the UTM coordinate system to within 0.25 pixel (7 m) accuracy using ground control points. Of the 198 channels, some overlap exists between the two radiometers and a number of channels are not calibrated resulting in 168 usable spectral channels.

4. Methods

4.1 *QuickBird data processing*

To reduce variability in spectral response, a simple forest/non-forest mask was generated from the four multi-spectral QuickBird bands using a supervised minimum distance classifier. The number of tree crowns with red attack damage was estimated using the ratio of red to green reflectance (Red-Green Index or RGI), which has been demonstrated as an effective approach for estimating the density of red attack crowns on the landscape. The RGI was computed and threshold values based on Coops *et al.* (2006) were used to discriminate between red attack and non attack tree crowns. This provided a complete census of red attack damage, consistently identified and fully georegistered to the Hyperion data.

4.2 *Detection of foliage moisture*

Several narrow-band indices have been developed to assess vegetation water content and these indices often ratio two wavelengths, with a band that is insensitive to water content as the numerator, and the water absorption feature either within the NIR or SWIR as the denominator. In this study, six moisture indices were calculated from the Hyperion data using the hyperspectral band closest to the centre of the liquid water absorption feature and a reference band as close as possible to the original band selection (Table 1). Some of the indices were developed specifically using Hyperion data (Roberts *et al.* 2003), while other indices were developed using hand-held spectrometers (Peñuelas *et al.* 1993, 1997), airborne hyperspectral data (AVIRIS) (Gao, 1996), or Landsat TM data (Hunt and Rock 1989; Hardisky *et al.* 1983). For each 30 by 30 m Hyperion pixel, the QuickBird forest/non-forest mask was used to estimate the proportion of forest vegetation within each pixel. For Hyperion pixels which had more than 95% forest, the proportion of the pixel classified as having red attack from an analysis of QuickBird RGI, was then compared to the spectral response in each of the moisture indices.

5. Results

Figure 2 shows the mean surface reflectances retrieved from Hyperion pixels that had varying degrees of red attack damage, as estimated from the QuickBird imagery. The general shape of the retrievals for increasing levels of infestation (no red attack damage, 5, 10, 15, 20, and 25% of the pixel with red attack damage) are similar. The Hyperion pixels with either no red attack damage (0%) or very low levels of red attack damage (0-5%) have more absorption in the chlorophyll absorbance region (680 nm), greater scattering in the NIR, and greater absorbance in the SWIR regions (Figure 2 insert). Alternatively, in the Hyperion pixels with a greater proportion of red attack damage, reflectance is greater in the visible and SWIR regions of the spectrum due to the lower availability of water and pigments in the red attack damaged tree crowns for absorption. The index with the strongest relationship to the proportion of red attack damage was the MSI (r^2 =0.51; $p < 0.001$) (Figure 3), followed by the NDII (r^2 =0.40; $p < 0.001$) (Figure 3). The greatest variability in both MSI and NDII values occurred in stands with no or minimal amounts of red attack damage and this may be attributable to the natural variability that is typical of lodgepole pine stands (Skakun *et al.* 2003)

6. Discussion and Summary

Measures of canopy reflectance collected by hyperspectral systems in the NIR and SWIR regions of the electromagnetic spectrum have been used to estimate canopy moisture (Carter 1991, Danson *et al.* 1992, Roberts *et al.* 2003), as both of these spectral regions exhibit pronounced water absorption features. All of the examined Hyperion moisture indices dependent on the 980 nm liquid water band (WBI, WI) had low correlations to the proportion of red attack damage in the Hyperion pixel, resulting from the low signal in this wavelength region (Ungar *et al.* 2003). Of the remaining indices considered, those with the largest correlation to the proportion of red attack damage in the Hyperion pixel were those indices which utilized the SWIR and NIR regions of the spectrum concurrently; the MSI and NDII both used 819 nm as the non-sensitive wavelength and either 1400 or 1650 nm as the water absorption wavelength. The variability in index

values for stands with no or minimal levels of red attack damage suggest that there is considerable natural variability in these stands, supporting the use of forest structural masks to constrain this variability. In contrast to the WBI and the WI, which were developed with hand-held spectrometers, the MSI was originally developed as a broad-band ratio (Landsat TM) that utilizes a combination of the moisture-affected SWIR bands and the theoretically unaffected NIR bands. The TCT Wetness index is a transformation of all Landsat TM or ETM+ spectral bands that is heavily weighted in the SWIR bands, but which also incorporates information from the visible and NIR (Huang *et al*. 2002). These results support the continued use of the TCT wetness index approach to detect mountain pine beetle red attack damage over large areas.

With respect to the strength of the Hyperion relationships, the results are encouraging in terms of the capacity of the Hyperion narrow-band widths to detect moisture stress. At the study site, the majority of Hyperion pixels had less than 20% of their total area (900 m^2) with red attack damage, which, depending on the size of the tree crowns, equates to approximately 15 or fewer damaged tree crowns. In areas where the Landsat EWDI has been applied successfully, the number of trees with red attack damage was often much larger – being in the order of 30 to 50 trees in a 900 m^2 area (Skakun *et al.* 2003). This suggests that space-borne hyperspectral imagery may have the capacity to detect lower densities of red attack damage at the landscape scale, which may allow for the earlier identification of small infestation centers, thereby aiding mitigation and control efforts. The capacity to detect low levels of mountain pine beetle red attack damage over large areas is a gap in the current data hierarchy used to monitor mountain pine beetle (Wulder et al., 2006c). As the first space borne hyperspectral sensor, Hyperion was designed as a research instrument; however, plans for the launch of space borne hyperspectral instruments (Shippert 2004) may present opportunities for detecting low levels of mountain pine beetle red attack damage over large areas.

Acknowledgements

This project is funded by the Government of Canada through the Mountain Pine Beetle Initiative, a six-year, $40 million program administered by Natural Resources Canada, Canadian Forest service. Doug Linton, Tony Ibaraki, and David Seemann are thanked for their efforts in collecting the field data. David Seemann and Sarah MacDonald are thanked for assistance with spatial analysis and image processing.

References

AMMAN, G. D., 1982, Characteristics of mountain pine beetles reared in four pine hosts. *Environmental Entomology*, **11**, pp. 590-593.

AMMAN, G.D., and COLE, W.E., 1983, *Mountain pine beetle dynamics in lodgepole pine forests. Part 2: Population dynamics*. USDA Forest Service, Ogden UT, GTR-INT-145, 59 p.

BIRK, R. J., STANLEY, T., SNYDER, G.I., HENNIG, T.A., FLADELAND, M.M. and POLICELLI, F., 2003, Government programs for research and operational uses of commercial remote sensing data. *Remote Sensing of Environment*, 88, pp. 3-16.

BRITISH COLUMBIA MINISTRY OF FORESTS, 1995, *Bark Beetle Management Guidebook*. Available online at : www.for.gov.bc.ca/tasb/legsregs/fpc/fpcguide/beetle/betletoc.htm (accessed March 31, 2005).

BRITISH COLUMBIA MINISTRY OF FORESTS AND RANGE, 2005, Mountain pine beetle affects 8.5 million hectares. Press Release: December 20, 2005. Victoria, British Columbia, Canada. Available on line at: http://www.for.gov.bc.ca/hfp/mountain_pine_beetle/2005mountain pine beetlesurvey.pdf (accessed March 31, 2005).

CARTER, G.A., 1991, Primary and secondary effects of water-content on the spectral reflectance of leaves. *American Journal of Botany*, **78**, pp. 916-924.

COLLINS, J.B. and WOODCOCK, C.E., 1996, An assessment of several linear change detection techniques for mapping forest mortality using multitemporal Landsat TM data. *Remote Sensing of Environment*, **56**, pp. 66-77.

COOPS, N.C., SMITH, M.L., MARTIN, M.M. and OLLINGER, S., 2003, Prediction of Eucalypt Foliage Nitrogen Content from Satellite Derived Hyperspectral Data. *IEEE Transactions on Geoscience and Remote Sensing*, **41**, pp. 1338- 1346.

COOPS, N.C., JOHNSON, M., WULDER, M.A., WHITE, J.C., 2006, Assessment of QuickBird high spatial resolution imagery to detect red-attack damage due to mountain pine beetle infestation. *Remote Sensing of Environment*, **103**, pp. 67-80.

CRIST, E. P., and CICONE, R.C., 1984, Application of the tasseled cap concept to simulated Thematic Mapper data. *Photogrammetric Engineering and Remote Sensing*, **50**, pp. 343-352.

DANSON, F. M., STEVEN, M. D., MALTHUS, T.J. and CLARK, J. A., 1992, High-spectral resolution data for determining leaf water-content. *International Journal of Remote Sensing*, **13**, pp. 461-470.

DATT, B., MCVICAR, T.R., VAN NIEL, T.G., JUPP, D. L. B., and PEARLMAN, J.S., 2003, Preprocessing EO-1 Hyperion hyperspectral data to support the application of agricultural indexes. *IEEE Transactions on Geoscience and Remote Sensing*, **41**, pp. 1246-1259.

GAO, B.C., 1996, NDWI - a Normalized Difference Water Index for Remote Sensing of Vegetation Liquid Water From Space. *Remote Sensing of Environment*, **58**, pp. 257-266.

HARDISKY, M.A., LEMAS, V. and SMART, R.M., 1983, The influence of soil salinity, growth form and leaf moisture on the spectral reflectance of Spartina alternifolia canopies. *Photogrammetric Engineering and Remote Sensing*, **49**, pp. 77-83.

HENIGMAN, J., EBATA, T., ALLEN, E., HOLT, J. and POLLARD, A., 1999, *Field Guide to Forest Damage in British Columbia*. (Victoria, British Columbia: British Columbia Ministry of Forests).

HILL, J.B., POOP, H.W. and GROVE, A.R. Jr., 1967, *Botany: A textbook for colleges*, 4th Edition. (Toronto: McGraw-Hill Book Co.)

HUANG, C., WYLIE, B., Yang, L., Homer, C. and Zylstra, G., 2002, Derivation of a tasselled cap transformation based on Landsat 7 at-satellite reflectance. *International Journal of Remote Sensing*, **23**, pp. 1741-1748.

HUNT, E. R. and ROCK, B. N., 1989, Detection of changes in leaf water-content using near-infrared and middle-infrared reflectances. *Remote Sensing of Environment*, **30**, pp. 43-54.

KAUTH, R.J. and THOMAS, G.S., 1976, The tasselled cap - A graphic description of the spectral-temporal development of agricultural crops as seen by Landsat. In *Symposium on Machine Processing of Remotely Sensed Data*, 29 June - 1 July 1976, Purdue University, West Lafayette, Indiana, pp. 4B-41-4B-51.

MATTHEW, M. W., ADLER-GOLDEN, S. M., BERK, A., RICHTSMEIER, S. C., LEVIN, R. Y., BERNSTEIN, L. S., ACHARYA, P. K., ANDERSON, G. P., FELDE, G. W., HOKE, M. P., RATKOWSKI, A., BURKE, H.-H., KAISER, R. D., and MILLER, D. P., 2000, Status of atmospheric correction using a MODTRAN4-based algorithm. In *SPIE Proceedings Algorithms for Multispectral, Hyperspectral, and Ultraspectral Imagery VI*, **4049**, pp. 199-207.

PEARLMAN, J.S., BARRY, P.S., SEGAL,C.C., SHEPANSKI, J., BEISO, D. and CARMAN, S.L., 2003, Hyperion, a space-based imaging spectrometer, *IEEE Transactions on Geoscience and Remote Sensing*, **41**, pp. 1160–1173.

PEÑUELAS, J., FILELLA, I., BIEL, C., SERRANO, L. AND SAVÉ, R., 1993, The reflectance at the 950–970 nm region as an indicator of plant water status. I *International Journal of Remote Sensing*, **14**, pp. 1887–1905.

PEÑUELAS, J., PINOL, J., OGAYA, R., FILELLA, I., 1997, Estimation of plant water concentration by the reflectance water index (WI (R900/R970)). *International Journal of Remote Sensing*, **18**, pp. 2869-2875.

REID, R.W., 1961, Moisture changes in lodgepole pine before and after attack by the mountain pine beetle. *Forestry Chronicle*, **37,** pp. 368-375.

ROBERTS, A., NORTHRUP, J. and LI, Y., 2004, *Mountain pine beetle detection and monitoring year two: Remote sensing detection procedures – 2002/2003 replication trials for early detection of spreading mountain pine beetle infestations*. Forest Investment Account (FIA) Land Based Investment Program Interim Report. FIA Project #2241004.

ROBERTS, D.A., DENNISON, P.E., GARDNER, M.E.,HETZEL, Y., USTIN, S.L., and LEE, C.T., 2003, Evaluation of the potential of Hyperion for fire danger assessment by comparison to the Airborne Visible/Infrared Imaging Spectrometer *IEEE Transactions on Geoscience and Remote Sensing*, **41**, pp. 1297-1310.

SAFRANYIK, L. and CARROLL, A.C., 2006, The biology and epidemiology of the mountain pine beetle in lodgepole pine forests. In *The Mountain Pine Beetle: A Synthesis of Biology, Management, and Impacts on Lodgepole Pine*, L. Safranyik and B. Wilson (Eds.), pp. 3-66 (Victoria, British Columbia: Canadian Forest Service, Natural Resources Canada).

SHIPPERT, P., 2004, Why use hyperspectral imagery? *Photogrammetric Engineering and Remote Sensing*, **70**, pp. 377-380.

SKAKUN, R. S., WULDER, M.A., and FRANKLIN, S.E., 2003, Sensitivity of the thematic mapper enhanced wetness difference index to detect mountain pine beetle red-attack damage. *Remote Sensing of Environment*, **86**, pp. 433-443.

UNGAR, S.G., PEARLMAN, J.S., MENDENHALL, J.A. and REUTER, D., 2003, Overview of the Earth Observing One (EO-1) mission, *IEEE Transactions on Geoscience and Remote Sensing*, **41**, pp. 1149-1159.

WHITE, J. C., WULDER, M.A., BROOKS, D., REICH, R. and WHEATE, R.D., 2005, Detection of red attack stage mountain pine beetle infestation with high spatial resolution satellite imagery. *Remote Sensing of Environment*, **96**, pp. 340-351.

WULDER, M. A., DYMOND, C.C., WHITE, J. C., LECKIE, D.G. and CARROLL, A.L., 2006a, Surveying mountain pine beetle damage of forests: a review of remote sensing opportunities. *Forest Ecology and Management*, **221**, pp. 27-41.

WULDER, M.A, WHITE, J.C., BENTZ, B., ALVAREZ, F. and COOPS, N.C., 2006b, Estimating the probability of mountain pine beetle red attack damage. *Remote Sensing of Environment*, **101**, pp. 150-166.

WULDER, M.A., WHITE, J.C., BENTZ, B., EBATA, T. 2006c. Augmenting the existing hierarchy for mountain pine beetle red-attack damage with satellite remotely sensed data. *Forestry Chronicle*, 82, pp. 187-202.

YAMAOKA, Y., SWANSON, R.H. and HIRATSUKA, Y., 1990, Inoculation of lodgepole pine with four blue-stain fungi associated with mountain pine beetle, monitored by a heat pulse velocity (HPV) instrument. *Canadian Journal of Forest Research*, **20**, pp. 31-36.

List of Tables and Figures

Table 1. A summary of moisture indices generated from the Hyperion data.

Index	Reference
Normalized Difference Infrared Index $NDII = \frac{\rho_{819} - \rho_{1649}}{\rho_{819} + \rho_{1649}}$	Hardisky et al (1983)
Moisture Stress Index $MSI = \frac{\rho_{1399}}{\rho_{819}}$	Hunt and Rock (1989)
Normalized Difference Water Index $NDWI = \frac{\rho_{837} - \rho_{1241}}{\rho_{837} + \rho_{1241}}$	Gao (1996)
Water Band Index $WBI = \frac{\rho_{900}}{\rho_{970}}$	Peñuelas *et al.* (1997)
Water Index $WI = \frac{R_{895}}{R_{972}}$	Peñuelas *et al.* (1993)
Modified Normalized Difference Water Index $mNDWI = \frac{\rho_{1070} - \rho_{1200}}{\rho_{1070} + \rho_{1200}}$	Roberts *et al.* (2003)

Figure 1. QuickBird imagery acquired over one of the forest stands in the study site on July 20, 2005. The QuickBird image is overlain with the 30 by 30 m Hyperion pixels (yellow). Individual tree crowns with mountain pine beetle red attack damage, as identified by a threshold of the Red Green Index, are delineated in red on the image.

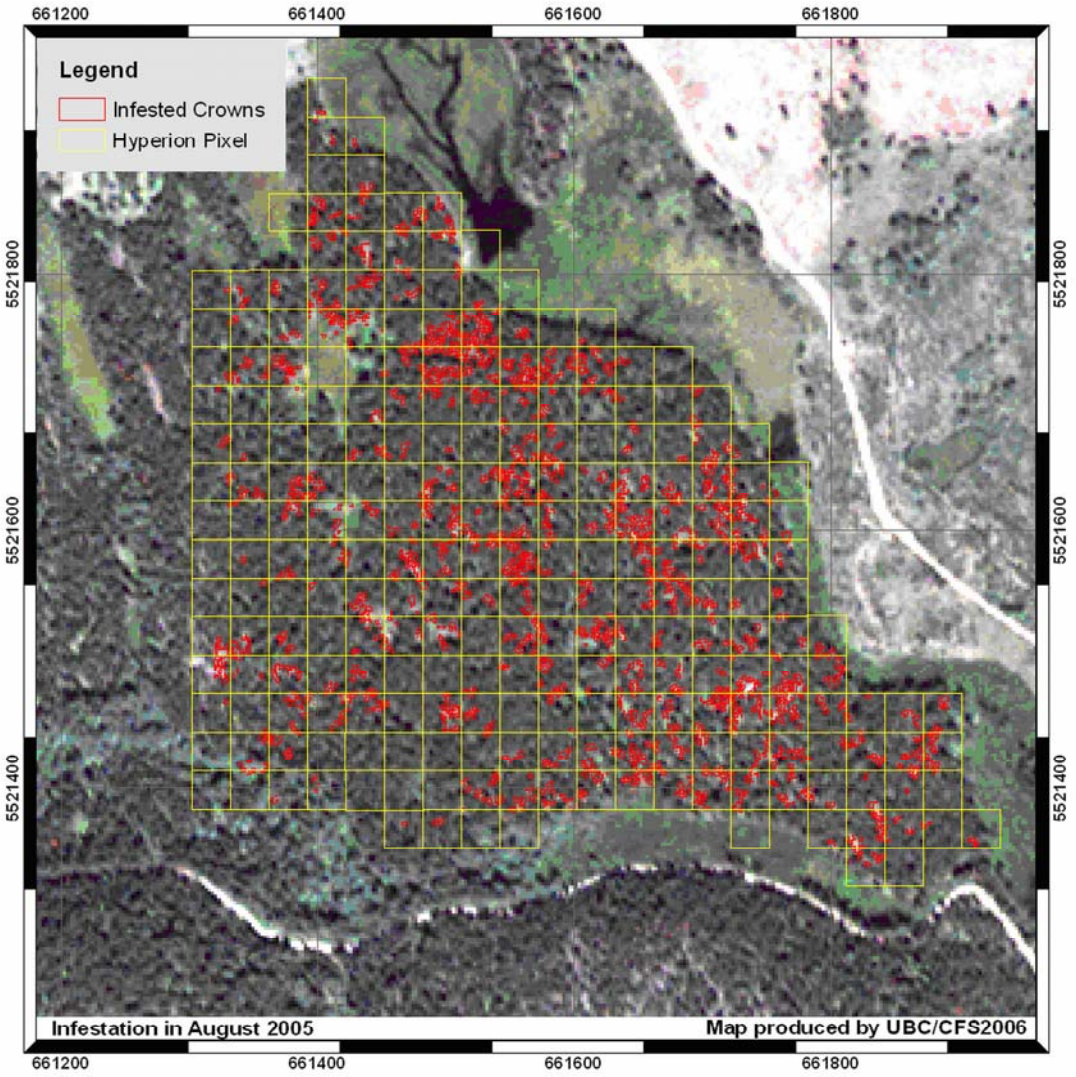

Figure 2. Spectral reflectance retrievals from all Hyperion bands for Hyperion pixels with increasing levels of mountain pine beetle red attack damage. The inset shows the primary water absorption region from 1477 to 1780 nm. In general, as the level of damage increases, the water content in the foliage decreases, and reflectance in the water absorption region increases.

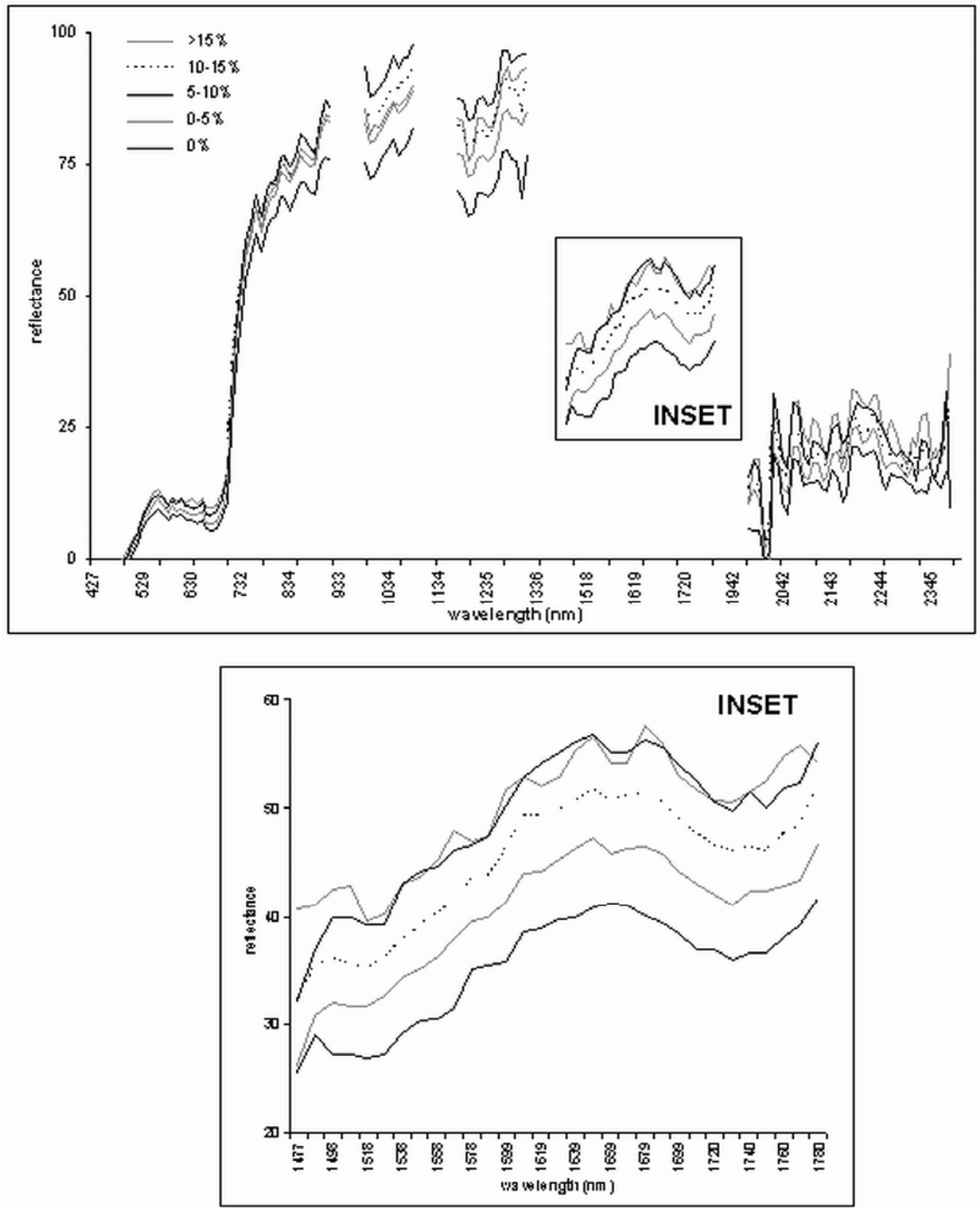

Figure 3. Relationship between the Moisture Stress Index (MSI) and the percentage of the Hyperion pixel with mountain pine beetle red attack damage (left). The same relationship is shown for the Normalized Difference Infrared Index (right).